

Effect of Monovalent Salt on Cationic Lipid Membranes As Revealed by Molecular Dynamics Simulations

Andrey A. Gurtovenko*

Laboratory of Physics and Helsinki Institute of Physics, Helsinki University of Technology, P.O. Box 1100, FI-02015 HUT, Finland, and Institute of Macromolecular Compounds, Russian Academy of Sciences, Bolshoi Prospect 31, V.O., St. Petersburg, 199004 Russia

Markus Miettinen and Mikko Karttunen

Biophysics and Statistical Mechanics Group, Laboratory of Computational Engineering, Helsinki University of Technology, P.O. Box 9203, FI-02015 HUT, Finland

Iipo Vattulainen

Laboratory of Physics and Helsinki Institute of Physics, Helsinki University of Technology, P.O. Box 1100, FI-02015 HUT, Finland, and Memphys—Center for Biomembrane Physics, Physics Department, University of Southern Denmark, Campusvej 55, DK-5230 Odense M, Denmark

Received: July 5, 2005

An atomic-scale understanding of cationic lipid membranes is required for development of gene delivery agents based on cationic liposomes. To address this problem, we recently performed molecular dynamics (MD) simulations of mixed lipid membranes comprised of cationic dimyristoyltrimethylammonium propane (DMTAP) and zwitterionic dimyristoylphosphatidylcholine (DMPC) (*Biophys. J.* **2004**, *86*, 3461–3472). Given that salt ions are always present under physiological conditions, here we focus on the effects of monovalent salt (NaCl) on cationic (DMPC/DMTAP) membranes. Using atomistic MD simulations, we found that salt-induced changes in membranes depend strongly on their composition. When the DMTAP mole fraction is small (around 6%), the addition of monovalent salt leads to a considerable compression of the membrane and to a concurrent enhancement of the ordering of lipid acyl chains. That is accompanied by reorientation of phosphatidylcholine headgroups in the outward normal direction and slight changes in electrostatic properties. We attribute these changes to complexation of DMPC lipids with Na⁺ ions which penetrate deep into the membrane and bind to the carbonyl region of the DMPC lipids. In contrast, at medium and high molar fractions of cationic DMTAP (50 and 75%) a substantial positive surface charge density of the membranes prevents the binding of Na⁺ ions, making such membranes almost insensitive to monovalent salt. Finally, we compare our results to the Poisson–Boltzmann theory. With the exception of the immediate vicinity of the bilayer plane, we found excellent agreement with the theory. This is as expected since unlike in the theoretical description the surface is now structured due to its atomic scale nature.

I. Introduction

Cationic liposomes, being one of the most promising nonviral vectors for gene delivery, allow one to overcome many disadvantages associated with the use of viral delivery agents such as toxicity and immunogenicity.^{1–4} However, while cationic lipids are nowadays widely used in molecular cell biology, they are still not as efficient as viral vectors. Their further development is hence highly desirable.

Atomic-scale molecular dynamics (MD) computer simulations have become a highly versatile tool for studying biomolecular systems. In particular, MD simulations can shed light on the atomistic details of the structure and dynamics of biomolecular systems. They complement experimental studies and, importantly, provide access to various static and dynamic properties not accessible by current experimental methods. It is therefore somewhat surprising that, as far as cationic membranes and their complexes with DNA are concerned, there are only two recent studies that have dealt with these issues.^{5,6} Bandyopadhyay et

al. studied the complexation of DNA with cationic lipids and the related DNA-induced effects in a cationic/zwitterionic equimolar membrane mixture.⁵ In a more recent study, Gurtovenko et al. considered a variety of mixed cationic/zwitterionic lipid membranes under salt-free conditions⁶ and showed that a variety of membrane properties depend on the fraction of cationic lipids in a membrane.

While the above works provide a good starting point for systematic studies of cationic membranes in atomic detail, they miss one key aspect that is an inherent part of both DNA–membrane complexes and, more generally, membranes under physiological conditions: the influence of salt. In particular, in complexes in which DNA is involved one should recall that a DNA molecule carries a large negative charge in its backbone, and is hence surrounded by cationic counterions. These counterions interact also with membranes, thus changing membrane properties before the complexation of DNA with cationic lipids actually starts. It is hence of considerable interest to clarify the interplay of cationic lipid membranes with salt.

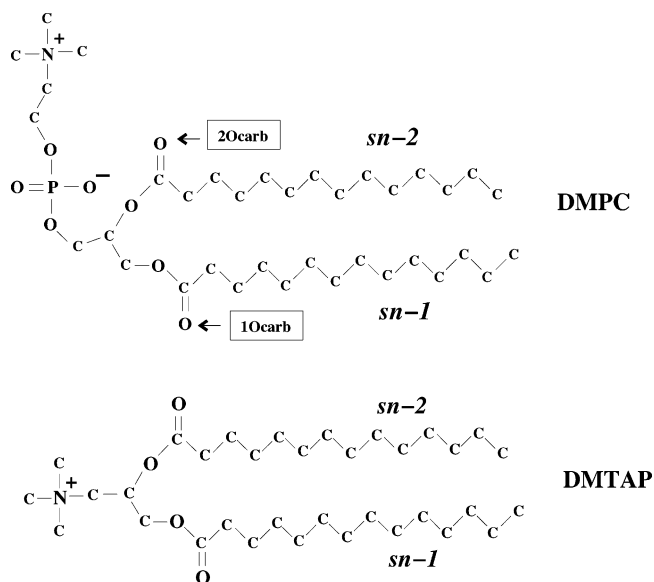


Figure 1. Chemical structures of a zwitterionic dimyristoylphosphatidylcholine (DMPC) and a cationic dimyristoyltrimethylammonium propane (DMTAP).

The understanding of salt-induced effects is slightly better for zwitterionic and anionic membranes. Recently, first atomistic MD simulations of zwitterionic phosphatidylcholine lipid bilayers with explicit salt were reported.^{7–10} It was found that monovalent cations alter both the structural and dynamical properties of zwitterionic membranes, leading to bilayer compression and enhanced ordering of lipid acyl chains and, consequently, to reduced lateral lipid mobility.⁷ MD simulations of anionic phosphatidylserine bilayers have further complemented the understanding of related issues.^{11–13} More generally, it is well-known that ions (in particular, cations) can adsorb onto lipid membranes and change their interfacial and electrostatic properties significantly. Experimental studies have shown that cations (especially, divalent ions) interact strongly with anionic lipids.^{14–17} This may be due to direct electrostatic attraction between cations and anionic lipid headgroups. However, salt ions are also known to influence membranes composed of zwitterionic phospholipids, the influence then being sensitive to the type of an ion and its valency.^{17–22} Furthermore, salt ions play a significant role in membrane fusion²³ and in transport properties across membranes.

The main objective of this study is to understand how monovalent salt affects the structural and electrostatic properties of mixed cationic/zwitterionic lipid membranes and how the effect of salt depends on membrane composition. As in our previous study,⁶ we employ classical atomistic MD simulations of zwitterionic dimyristoylphosphatidylcholine (DMPC) and cationic dimyristoyltrimethylammonium propane (DMTAP) bilayers; see Figure 1. These lipids have the same nonpolar hydrocarbon chains and differ only by their headgroups. Such DMPC/DMTAP binary lipid mixtures have been studied experimentally in the presence of DNA^{24–27} as well as through computer simulations.⁵

To study the effects of salt, we varied the NaCl concentration in three different DMPC/DMTAP membrane mixtures. We show that monovalent salt affects the structural properties of cationic membranes. When the DMTAP fraction is small, monovalent salt plays a prominent role and has a strong influence on membrane properties through binding of sodium ions to the carbonyl region of zwitterionic DMPC. The resulting formation of complexes of DMPC lipids with Na⁺ ions leads to an

enhanced packing of lipids, which in turn leads to a variety of further changes in bilayer properties. In contrast, at medium and high DMTAP concentrations a large positive surface charge at a membrane–water interface prevents the binding of Na⁺ ions to DMPC lipids, and monovalent salt is found to have only a minor effect.

II. Model and Simulation Details

Zwitterionic DMPC and cationic DMTAP were used for atomistic simulations of lipid bilayer mixtures under the influence of monovalent NaCl salt. DMPC and DMTAP were described by a united atom representation in terms of 46 and 39 interaction sites, respectively; see Figure 1. Force field parameters for the lipids are based on the united atom force field of Berger et al.²⁸ This description has been previously validated for PC lipid bilayers^{29,30} against experimentally observed values for the area and volume per lipid.³¹ The force field parameters for DMPC and DMTAP are available on-line at <http://www.softsimu.org/downloads.shtml>. For water we used the SPC water model.³² For NaCl we employed the default set of parameters supplied within the Gromacs force field,^{33,34} while being aware of the effects of different models for sodium and chloride ions.³⁵

The Lennard-Jones interactions were cut off at 1 nm without shift or switch functions. Since truncation of electrostatic interactions is known to lead to pronounced artifacts in simulations of lipid bilayers,^{36–38} the long-range interactions were handled using the particle-mesh Ewald (PME) method.^{39,40} All simulations were performed in the NpT ensemble at 323 K and 1 bar. Temperature was chosen such that the lipid bilayers were in the liquid-crystalline phase (for a DMPC/DMTAP binary mixture the main transition temperature has a maximum of about 310 K at $\chi_{\text{TAP}} \approx 0.45$, see ref 26). A Berendsen thermostat with a coupling time constant of 0.1 ps and a Berendsen barostat⁴¹ with a coupling time constant of 1.0 ps were employed. All lipid bond lengths were constrained using the LINCS algorithm,⁴² while SETTLE⁴³ was used for water. The bilayers were set to align in the xy -plane. The equations of motion were integrated with a time step of 2 fs. All simulations were performed using the GROMACS suite.^{33,34}

We considered three different binary mixtures of DMPC and DMTAP with a varying molar fraction of cationic DMTAP (χ_{TAP}): 0.06, 0.50, and 0.75. As the starting point, we used the final, equilibrated structures of DMPC/DMTAP bilayers from our previous study without salt.⁶ They are available at <http://www.softsimu.org/downloads.shtml>. These bilayers consisted of 128 lipids, ~3600 water molecules, and Cl⁻ counterions to neutralize the positive charges of the DMTAP lipids. Since salt ions are able to bind to water molecules and, consequently, to decrease the hydration level of lipids, the number of water molecules was increased here by a factor of 1.5. The resulting bilayers contained ~5100 ($\chi_{\text{TAP}} = 0.06$) to ~5500 ($\chi_{\text{TAP}} = 0.75$) water molecules. They were used as initial configurations in our present salt-free bilayer simulations, which were performed to serve as a reference for studying salt effects.

To study the effects of salt, all three salt-free systems were first preequilibrated for 20 ns. Randomly chosen water molecules were then replaced by Na⁺ and Cl⁻ ions. We studied three different NaCl concentrations for each bilayer: 0.1, 0.5, and 1.0 M. To implement this, 9–96 pairs of Na⁺ and Cl⁻ ions were added.

In total, we simulated 12 bilayers (3 DMPC/DMTAP mixtures at 4 salt concentrations including salt-free systems). Each system had more than 21 000 atoms. Cationic lipid bilayers with salt

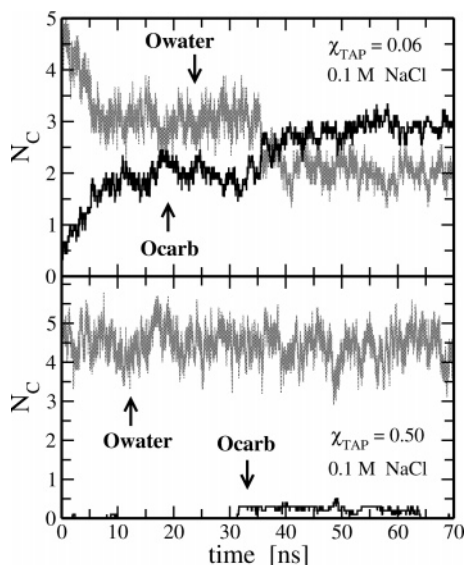


Figure 2. Time evolution of coordination numbers N_C of sodium ions bound to carbonyl oxygens of DMPC or to water oxygens. Results are shown for molar fractions $\chi_{\text{TAP}} = 0.06$ (top) and $\chi_{\text{TAP}} = 0.50$ (bottom). NaCl concentration is 0.1 M in both cases.

were simulated for 70 ns each, while for salt-free systems the times ranged from 50 to 60 ns. Only the last 20 ns of the trajectories were used for analysis (see next section). As a critical test, one of the simulations (an equimolar DMPC/DMTAP mixture with 0.5 M of NaCl) was extended to 200 ns. The combined simulation time of all simulation runs exceeds 0.9 μs . Each simulation was run in parallel over four processors on an IBM eServer Cluster 1600 system or on a cluster of 3.2 GHz Pentium 4 CPUs.

III. Results and Discussion

A. Equilibration and Ion Binding. Equilibration is of concern in all MD simulations of membrane systems. This is particularly true if salt is present, since, from computational perspective, the time scales involved may become substantial. This is well demonstrated by recent studies by Böckmann et al., who found that the association of ions with PC headgroups is a slow process with typical time scales ranging from 20 to 100 ns depending on the nature of salt used.^{7,8}

For salt-free membranes we used the standard approach and computed the area per lipid to monitor equilibration. Even in these salt-free cases, however, we found that the equilibration of counterions with respect to the headgroup region is slow: 30 ($\chi_{\text{TAP}} = 0.06$ and $\chi_{\text{TAP}} = 0.75$) to 40 ns ($\chi_{\text{TAP}} = 0.50$) is needed for the area per lipid to become stable (data not shown). For systems with salt the equilibration takes even longer. As demonstrated in recent computational studies,^{7,8} the slowest processes in phosphatidylcholine lipid bilayers with monovalent salt are associated with the binding of sodium ions to the lipid carbonyl region. Therefore, to monitor equilibration in simulations with salt, we measured the coordination numbers of Na^+ ions with lipid carbonyl and water oxygens.

In Figure 2 we show the time evolution of sodium ion–DMPC carbonyl oxygen coordination numbers, N_C (denoted as 1Ocarb and 2Ocarb, see Figure 1), as well as those for sodium ions and water oxygens. The results are shown for small ($\chi_{\text{TAP}} = 0.06$) and intermediate ($\chi_{\text{TAP}} = 0.5$) DMTAP molar fractions in aqueous solution with 0.1 M of NaCl. The coordination numbers of Na^+ ions with DMTAP carbonyl oxygens are not shown because we did not find any noticeable binding of sodium

ions to them. This may be due to the chemical structure of DMTAP: the binding of Na^+ is prevented by the cationic TAP headgroup located rather close to the carbonyl region of lipid chains; see Figure 1. Coordination numbers presented in Figure 2 were calculated by counting the total numbers of target oxygens within the first coordination shell of a sodium ion. The radius of the shell was set to 0.31 nm, as obtained from the corresponding radial distribution functions.

As seen in Figures 2 (top) and 3 (top) the sodium ions bind to DMPC carbonyl oxygens when the DMTAP fraction is small ($\chi_{\text{TAP}} = 0.06$). For Na^+ ions this process is accompanied by loss of water molecules from their first hydration shell as illustrated in Figure 2 (top). The overall picture here is reminiscent to that found in previous studies^{7,8} for zwitterionic PC lipid bilayers with monovalent salt and, to a smaller extent, also with ref 9. Additionally, a similar binding of sodium counterions to the ester lipid region was found in a recent MD study of anionic phosphatidylserine bilayers.¹³ An exponential fit to the curves in Figure 2 (top) gives sodium binding times of 32 and 26 ns for DMPC carbonyl and water oxygens, respectively, for 0.1 M salt. Increasing the salt concentration speeds up the binding: for the Na–Ocarb coordination number the same exponential fit yields binding times of 17 and 10 ns for salt concentrations of 0.5 and 1.0 M, respectively (data not shown). Nevertheless, we decided to consider the first 50 ns as an equilibration period for *all* bilayer simulations with NaCl, using the last 20 ns (out of 70 ns) for subsequent analysis.

The situation changes completely when the DMTAP concentration is increased to an intermediate value, $\chi_{\text{TAP}} = 0.5$. Then, sodium ions do *not* bind to the carbonyl region of the DMPC lipids, and correspondingly, they do *not* lose water from their first hydration shells; see Figure 2 (bottom) and also Figure 3 (bottom). Since half of all lipids are now cationic, the most plausible explanation is that a large positive surface charge of the bilayer is responsible for such behavior. As a critical test of this finding, for an equimolar DMPC/DMTAP mixture ($\chi_{\text{TAP}} = 0.5$) with 0.5 M of NaCl, we extended our simulations up to 200 ns. We did not find any noticeable and stable binding of sodium ions to the DMPC carbonyl region. The same picture also emerges for cationic membranes with high DMTAP concentration, $\chi_{\text{TAP}} = 0.75$ (data not shown).

Now, let us discuss the binding of Na^+ ions to cationic membranes at $\chi_{\text{TAP}} = 0.06$ in more detail. The coordination numbers of sodium ions with DMPC carbonyl oxygens in Figure 2 were calculated by averaging over all Na^+ ions. To obtain the average number of DMPC lipids bound to a sodium ion, one needs only to average over sodium ions having PC carbonyl oxygens in their first coordination shells. Such an averaging shows that 3.24 ± 0.15 , 2.69 ± 0.14 , and 2.89 ± 0.18 DMPC lipids are bound, on the average, to a sodium ion when the salt concentrations are 0.1, 0.5, and 1.0 M, respectively. These average values of coordination numbers for Na–Ocarb pairs can, however, vary significantly within the bilayer, as is illustrated in Figure 4 for a bilayer with 0.5 M salt. It is clear that when a sodium ion penetrates deep into the cationic membrane ($z < 2$ nm) it binds to PC carbonyl oxygens and, at the same time, loses its coordinated water as well as Cl^- ions. The maximal value of the coordination number for Na–Ocarb is about 3.0 at $z = 1$ nm, i.e., larger than the average value of 2.69; see Figure 4.

The obtained average values for coordination numbers of Na–Ocarb pairs mean that a sodium ion binds on average to roughly *three* DMPC lipid molecules (no binding of sodium ions to DMTAP lipids was observed). This finding is in agreement with

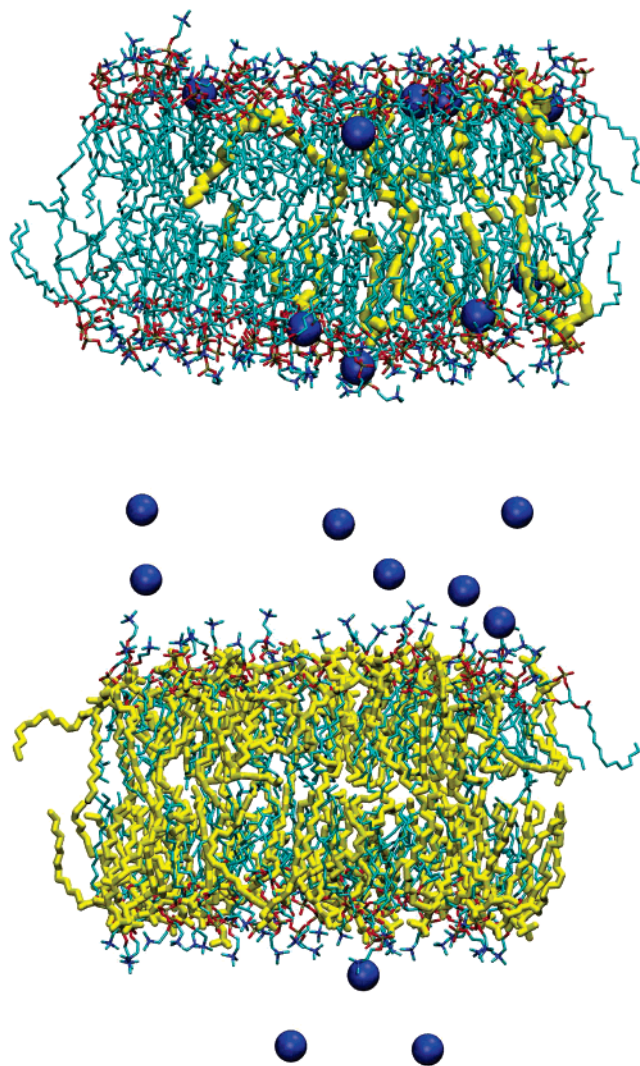


Figure 3. (top) Structure of the DMPC/DMTAP bilayer after 70 ns with 0.1 M NaCl and $\chi_{\text{TAP}} = 0.06$. Lipids shown are DMPC (cyan) and DMTAP (yellow). Sodium ions are shown as blue spheres. Water is not shown. (bottom) Corresponding structure for an intermediate DMTAP fraction, $\chi_{\text{TAP}} = 0.50$.

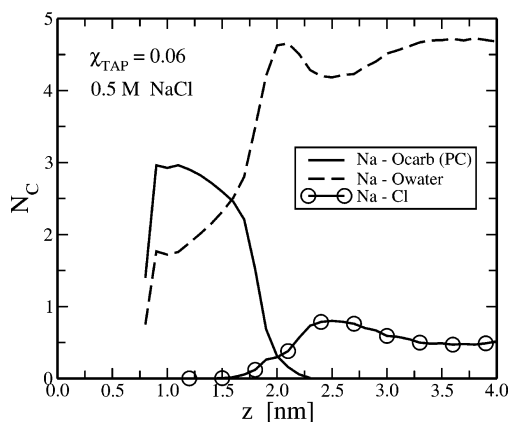


Figure 4. Average coordination numbers N_C of sodium ions with DMPC carbonyl oxygens (solid line), with water oxygens (dashed line), and with Cl^- ions (line with circles). Results are shown as a function of distance z from the bilayer center for a cationic membrane with $\chi_{\text{TAP}} = 0.06$, the NaCl concentration being 0.5 M.

recent computational results⁷ for POPC lipid bilayers in aqueous solutions with monovalent salt. Another recent MD study devoted to effects of NaCl on DPPC lipid bilayers⁹ revealed

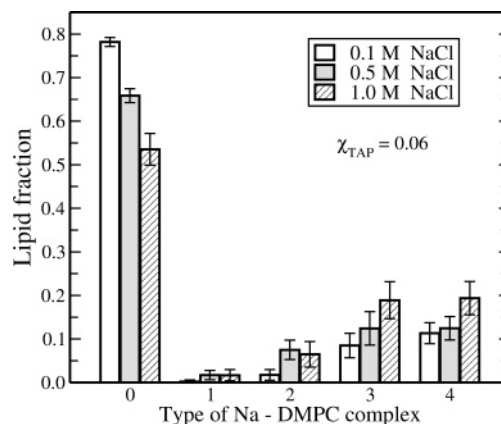


Figure 5. Average fractions of DMPCs involved in various sodium–lipid complexes for cationic membranes at $\chi_{\text{TAP}} = 0.06$: “0”, DMPCs are not bound to sodium ions; “1”, one sodium ion binds to a single DMPC; “2”, one sodium ion forms a complex with two DMPCs, etc. The error bars are computed as standard deviations.

the binding of a sodium to two lipid molecules only. This discrepancy may be caused by the shorter simulation times (10 ns) employed in ref 9.

The above “averaged” picture of the binding of a Na^+ ion to three PC lipids is, however, oversimplified. A more detailed analysis of the sodium–lipid complexation reveals a broad distribution of DMPC lipids over complexes of various types; see Figure 5. First, a substantial fraction of DMPC lipids is not involved in Na–DMPC complexes at all. That fraction systematically decreases with increasing salt concentration from 0.78 (0.1 M NaCl) to 0.54 (1.0 M NaCl). Second, the main contribution to Na–DMPC complexation is provided by complexes of *three* and *four* DMPC lipids. At 0.1 M NaCl the complexes of four lipids dominate slightly over those formed by three lipids. This, along with the fact that contributions of Na–DMPC complexes with one and two lipids are negligible, leads to a rather large value of the average coordination number (3.24) for Na–Ocarb pairs. At higher NaCl concentrations, the contributions from complexes formed by three and four lipids are the same. At 0.5 M NaCl, a relatively large fraction of lipids involved in complexes with two lipids decreases the average value of coordination number for Na–Ocarb as compared to that for the bilayer system with 1.0 M salt (2.69 vs 2.89). It is noteworthy that for a cationic membrane with 1.0 M NaCl the observed *average* binding of a Na^+ ion to ~ 3 DMPC lipids is caused not only by the formation of complexes involving three lipids but also by the presence of lipids organized in complexes consisting of four and two lipids, such lipids being present in the bilayer in an approximate ratio 2:1. We note that a rather broad distribution of PC lipids over various complexes with sodium ions was also found in pure DMPC lipid bilayers under the influence of monovalent salt.¹⁰

B. Structure of Lipid Bilayers. The DMTAP-content-dependent binding of sodium ions found for DMPC/DMTAP membranes means that the effect of monovalent salt on structural membrane properties depends on the concentration of cationic lipids. Adding monovalent salt to a cationic bilayer leads to a pronounced decrease in the area per lipid for a bilayer with a small cationic lipid content ($\chi_{\text{TAP}} = 0.06$). For medium and high DMTAP fractions ($\chi_{\text{TAP}} \geq 0.5$) the average area per lipid is only weakly affected; see Figure 6. For salt-free bilayers the area per lipid depends nonmonotonically on DMTAP fraction, as discussed in our previous study.⁶ An even stronger non-monotonic dependence has been observed in monolayer studies using cationic lipids.⁴⁴ The overall compression of a cationic

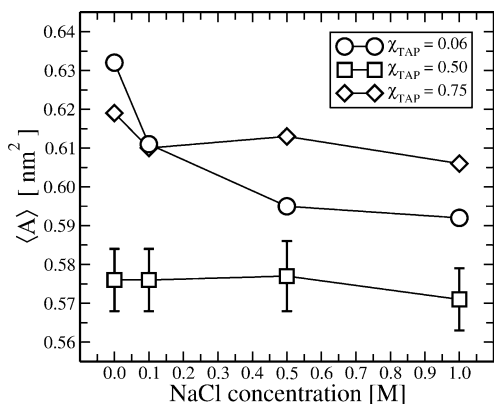


Figure 6. Average area per lipid, $\langle A \rangle$, as a function of NaCl concentration for all χ_{TAP} considered. Typical standard deviations in $\langle A \rangle$ are shown for bilayer systems with $\chi_{\text{TAP}} = 0.50$.

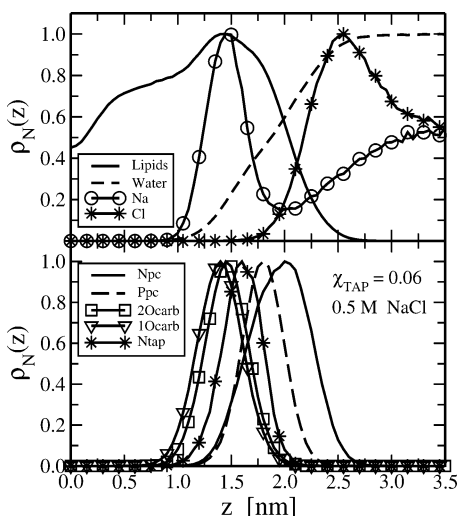


Figure 7. Scaled number densities $\rho_N(z)$ for a DMPC/DMTAP bilayer at $\chi_{\text{TAP}} = 0.06$ and NaCl concentration of 0.5 M: (top) number density profiles for lipids, water, sodium ions, and chloride ions; (bottom) number density profiles for DMPC nitrogens, DMPC phosphorus atoms, DMPC carbonyl oxygens 2Ocarb and 1Ocarb, and DMTAP nitrogens. The case of $z = 0$ corresponds to the bilayer center.

membrane with $\chi_{\text{TAP}} = 0.06$ is about 6.5% in area (from $0.632 \pm 0.09 \text{ nm}^2$ for a salt-free system to $0.592 \pm 0.07 \text{ nm}^2$ for a system with 1.0 M salt). This compression, also reported in MD studies of neat PC lipid bilayers under the influence of monovalent salt,^{7,9,10} can be attributed to a more compact packing of DMPC lipids because of the formation of lipid–sodium complexes.

Locations of various groups of lipids and salt ions can be visualized through number density profiles. That is shown in Figure 7 (scaled by their maximal values for clarity) for $\chi_{\text{TAP}} = 0.06$ and 0.5 M NaCl. Binding of sodium ions to the membrane is now clearly seen: sodium ions penetrate deep into the DMPC carbonyl region, and their number density peak coincides almost exactly with those of DMPC carbonyl oxygens, 1Ocarb and 2Ocarb; see Figure 7. We also note that carbonyl oxygens of *sn*-1 PC acyl chains (1Ocarb) are located deeper in the bilayer than those of *sn*-2 PC chains (2Ocarb); see Figure 7 (bottom). The 2Ocarb oxygens are, therefore, more easily accessible to sodium ions, and hence the Na⁺ ions bind mostly to the *sn*-2 DMPC carbonyl oxygens (data not shown). In turn, as Figure 7 (top) demonstrates, most of the chloride ions are mainly located in bulk water about 0.5–1 nm from the water–membrane interface.

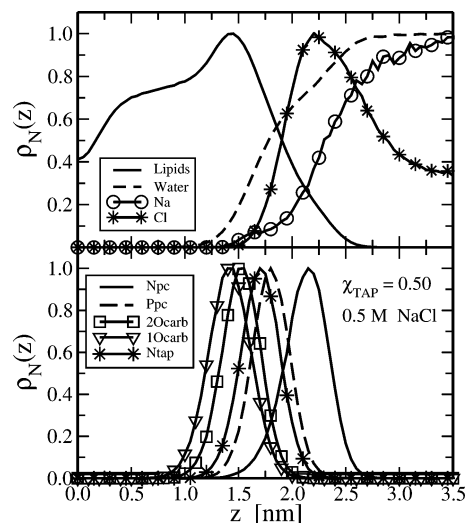


Figure 8. Scaled number densities $\rho_N(z)$ for a cationic bilayer with $\chi_{\text{TAP}} = 0.5$ in aqueous solution with 0.5 M NaCl. Curves are marked in the same way as those in Figure 7.

The situation is different for bilayers with medium and high DMTAP content; see Figure 8. Sodium ions do not penetrate into the membrane but are located in bulk water instead. Chloride ions are also in bulk water but they get closer to the water–membrane interface than they do for $\chi_{\text{TAP}} = 0.06$; see Figure 7 (top). That is due to slightly enhanced binding of Cl⁻ ions to DMPC nitrogens and, to a smaller extent, to TAP headgroups. Note that the distance between the number density peaks of phosphorus and nitrogen atoms of DMPC headgroups increases as DMTAP fraction increases (Figures 7 (bottom) and 8 (bottom)). That is a sign of a DMTAP-induced reorientation of the PC headgroups.⁶ Thus, the above difference in the Na⁺ binding for cationic membranes of different DMPC/DMTAP compositions is clearly observed also from the number density profiles.

C. Ordering of Lipid Acyl Chains and Orientation of Zwitterionic Lipid Headgroups. The changes in $\langle A \rangle$ for membranes with small cationic lipid content (Figure 6) are related to the ordering of lipid chains characterized by the deuterium order parameter S_{CD}

$$S_{\text{CD}} = \frac{1}{2} \langle 3 \cos^2 \theta - 1 \rangle \quad (1)$$

Here θ is the angle between the CD bond and the bilayer normal, and the brackets denote averaging over time and lipid molecules. In our united-atom model the positions of the deuterium atoms are not available; they, however, can be reconstructed from the positions of three successive carbons under assumption of ideal tetrahedral geometries of CH₂ groups.^{45,46}

In Figure 9 we plot the deuterium order parameter $|S_{\text{CD}}|$ averaged over *sn*-1 and *sn*-2 chains for DMPC and DMTAP for $\chi_{\text{TAP}} = 0.06$. It is seen that the behavior of $|S_{\text{CD}}|$ is well correlated with that of the area per lipid (see Figure 6): adding monovalent salt to a cationic membrane having a small DMTAP fraction leads to a compression of the membrane and, correspondingly, enhances the ordering of the acyl chains. This finding is in agreement with computational studies of pure PC lipid bilayers under influence of NaCl.^{7,9} In contrast to the case $\chi_{\text{TAP}} = 0.06$, the order parameter $|S_{\text{CD}}|$ turns out to be almost insensitive to the presence of salt for cationic bilayers with higher DMTAP fractions, Figure 10.

To further illustrate the effects of salt on the ordering of the acyl chains, we calculated the average value of $|S_{\text{CD}}|$ for the

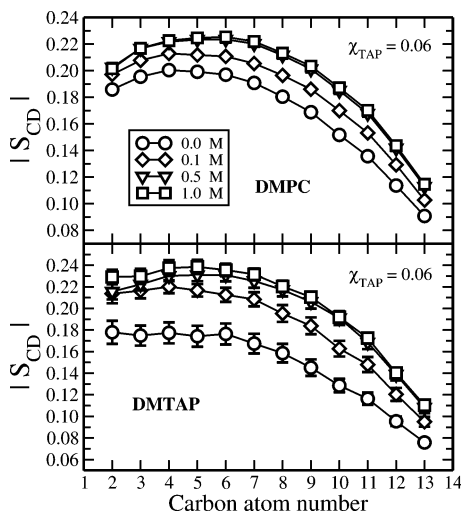


Figure 9. Deuterium order parameter $|S_{CD}|$ averaged over *sn*-1 and *sn*-2 chains for DMPC (top) and DMTAP (bottom) at $\chi_{TAP} = 0.06$. The numbering of carbon atoms starts from the ester region. The error bars are computed by splitting trajectories into 10 pieces of 2 ns each. The error bars for $|S_{CD}|$ of DMPC (top) are of the same size as the symbols.

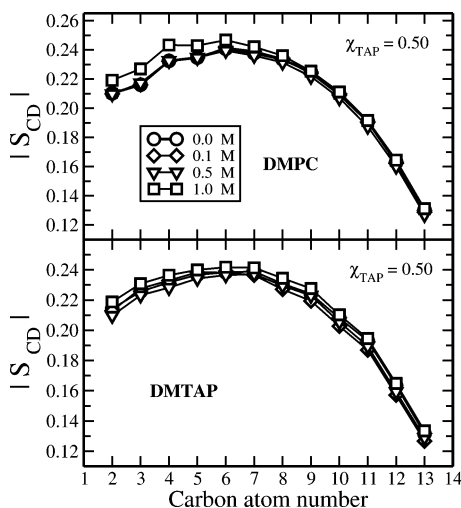


Figure 10. Deuterium order parameter $|S_{CD}|$ averaged over *sn*-1 and *sn*-2 chains for DMPC (top) and DMTAP (bottom) at $\chi_{TAP} = 0.50$. The error bars are of the same size as the symbols.

first seven hydrocarbons (from C2 to C8). This “plateau” order parameter S_{ave} is plotted in Figure 11 separately for DMPC and DMTAP lipids. Again, we find a clear connection between changes in S_{ave} and $\langle A \rangle$ upon adding salt. Smaller area per lipid corresponds to a larger “plateau” order parameter and vice versa. The influence of salt on the “plateau” order parameter S_{ave} of bilayer systems with $\chi_{TAP} = 0.06$ is very pronounced, while bilayers with $\chi_{TAP} \geq 0.5$ demonstrate only slight changes in S_{ave} .

A closer inspection of Figure 11 shows interesting features with regard to changes in S_{ave} for cationic membranes with $\chi_{TAP} = 0.06$. For a salt-free bilayer system, DMTAPs are more disordered than DMPCs. This is in agreement with our previous study; see Figure 6 of ref 6. When salt is added, the overall area of the membrane decreases and the ordering of acyl chains of *both* DMPC and DMTAP is enhanced. It is interesting, however, that this enhancement in $|S_{CD}|$ turns out to be higher for DMTAPs (which do *not* form complexes with Na^+) than that for DMPCs. At all nonzero salt concentrations the value of S_{ave} of DMTAPs exceeds that of DMPCs; see Figure 11.

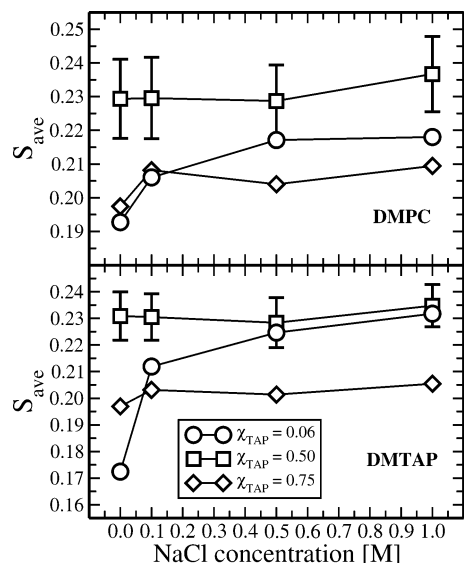


Figure 11. Plateau order parameter S_{ave} calculated by averaging S_{CD} over C2 to C8 hydrocarbons. Shown are results for DMPC (top) and DMTAP (bottom) as a function of NaCl concentration. Typical standard deviations are shown for bilayer systems with $\chi_{TAP} = 0.50$.

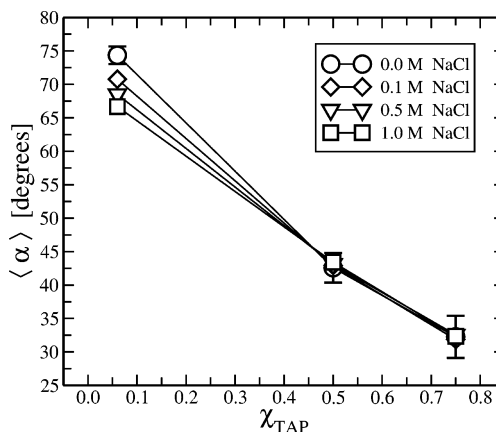


Figure 12. The average angle $\langle \alpha \rangle$ between the P–N vector of a DMPC lipid headgroup and the bilayer normal as a function of χ_{TAP} . Typical standard deviations are shown for salt-free systems.

Of particular interest is also the orientation of zwitterionic DMPC headgroups which possess a dipole moment along the P–N vector, see Figure 1, and, therefore, contribute to the electrostatic potential across the membrane. In Figure 12 we plot the average angle $\langle \alpha \rangle$ between the P–N vector of the DMPC headgroup and the outward bilayer normal for all bilayer systems considered. When DMTAP fraction is small ($\chi_{TAP} = 0.06$), the addition of monovalent salt leads to a clear ($\approx 7.5^\circ$) reorientation of the PC headgroups out of the bilayer. A similar effect has been found for pure phosphatidylcholine bilayers with salt.^{7,10} For larger DMTAP fractions ($\chi_{TAP} = 0.5$ and $\chi_{TAP} = 0.75$) salt has no effect on the PC headgroup orientation; see Figure 12. In addition to the effects of salt, we would like to point out that at high DMTAP concentrations the DMPC headgroups are already reoriented considerably due to their coordination with DMTAP headgroups.⁶

D. Electrostatic Potential and Surface Charge Density. For each bilayer system we computed charge densities of various bilayer components. In general, the charge density profiles follow rather closely the number densities: for small DMTAP concentrations the positive charges of DMTAP and Na^+ bound to DMPC are compensated by the phosphate groups of DMPC. For large χ_{TAP} , positive charges of DMTAP are compensated

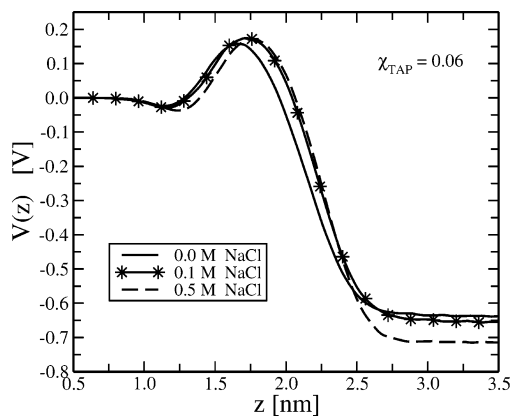


Figure 13. Electrostatic potential $V(z)$ across a membrane having $\chi_{\text{TAP}} = 0.06$. Systems: 0.0 M (solid line), 0.1 M (stars), and 0.5 M (dashed line) of NaCl. The potential was set to zero at the bilayer center. Potential for a bilayer with 1.0 M of NaCl is essentially identical with the 0.5 M case and is not shown here.

by phosphate groups of DMPC as well as by water molecules and chloride ions. Then, sodium ions are mostly neutralized by chloride ions in bulk water.

The electrostatic potential $V(z)$ across a monolayer was calculated by integrating twice over the charge densities. We found that adding monovalent salt to a cationic membrane with low cationic lipid content leads to a slight increase of the overall electrostatic potential across the monolayer; see Figure 13. The increase depends on salt concentration and saturates at 0.5 M NaCl, being around 80 mV. This finding qualitatively agrees with results for pure PC lipid bilayers with salt^{7,9,10} and can be attributed to the reorientation of the DMPC headgroups (cf. Figure 12). The electrostatic potential of cationic bilayers with higher DMTAP fractions, $\chi_{\text{TAP}} \geq 0.50$, for which salt does not change the *average* P–N vector orientation, remains unchanged as compared to the $V(z)$ of corresponding salt-free bilayer systems; see Figure 12 in ref 6.

Since cationic membranes possess a substantial positive surface charge, it is interesting to explore how monovalent salt affects the electric surface properties of membranes. In practice, a lipid bilayer cannot be thought of as being an ideal planar charged surface because of the broad interface region and a rough interface. Therefore, the surface charge profile of a lipid bilayer has to vary significantly within the bilayer. In this work the surface charge density $\sigma(z)$ as a function of distance z from the bilayer center was calculated as

$$\sigma(z) = \int_0^z \rho(z') dz' \quad (2)$$

where $\rho(z)$ is the charge density of the cationic bilayer *excluding water*.⁹ In Figure 14 we plot $\sigma(z)$ for all bilayer systems considered. As a common feature, the surface charge density is negative in the vicinity of nonpolar hydrocarbon chains, and all surface charge density curves demonstrate a minimum around $1.4 \text{ nm} < z < 1.75 \text{ nm}$. Further away from the bilayer center, $\sigma(z)$ becomes positive and has a maximum close to the outer border of the membrane–water interface. Thus, bulk water “sees” a cationic membrane essentially as a positively charged surface.

The shapes of the $\sigma(z)$ curves as well as changes induced in $\sigma(z)$ by salt are found to differ considerably for all DMTAP fractions studied. When a cationic lipid content is small, the region where $\sigma < 0$ is extensive and characterized by a deep minimum; see Figure 14 (top). The main contribution to $\sigma(z)$ in this domain is mainly due to DMPCs. Their surface charge density is found to be always negative.⁹ Upon addition of salt,

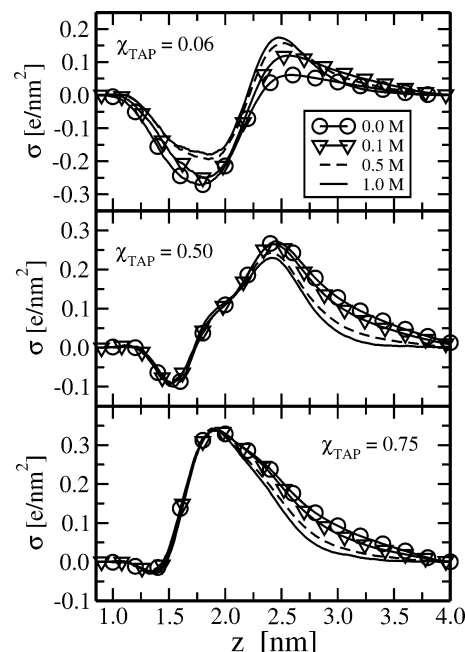


Figure 14. Surface charge density $\sigma(z)$ as a function of distance z from the bilayer center for membranes with $\chi_{\text{TAP}} = 0.06$ (top), $\chi_{\text{TAP}} = 0.5$ (middle), and $\chi_{\text{TAP}} = 0.75$ (bottom), at different NaCl concentrations.

sodium ions penetrate deep into the membrane (up to $z \sim 1.5 \text{ nm}$) and their positive charge leads to the shift of $\sigma(z)$ curves toward larger values along the σ -axis.

In contrast, for $\chi_{\text{TAP}} = 0.5$ the domain in which $\sigma < 0$ is much more constrained, and the minimum of $\sigma(z)$ is less pronounced than that in $\chi_{\text{TAP}} = 0.06$. Evidently, this is due to the DMTAPs. Since sodium ions do not bind to DMPC at higher DMTAP fractions, the domain of negative surface charge is not affected by salt. However, increasing salt concentration slightly reduces the peak height of $\sigma(z)$ in the domain where $\sigma > 0$; see Figure 14 (middle). This effect may be explained by the enhanced screening of positive charges of cationic DMTAP due to a growing population of Cl^- ions.

For $\chi_{\text{TAP}} = 0.75$, the domain $\sigma < 0$ almost disappears because cationic DMTAPs dominate and the surface charge density is positive almost everywhere in the interface region; see Figure 14 (bottom). The height of the peaks of $\sigma(z)$ turns out to be insensitive to salt. Screening of positive charges of the DMTAPs by Cl^- ions may be responsible for this, since such a screening is substantial even for salt-free systems.⁶ Indeed, as seen in Figure 15 (bottom) the coordination numbers of TAP headgroups with chloride ions are close to unity for a cationic bilayer with $\chi_{\text{TAP}} = 0.75$, even when only Cl^- counterions are present (0.0 M NaCl). In other words, positive charges of the TAP headgroups are almost fully screened by Cl^- ions before salt is added. Furthermore, Figure 15 shows that Cl^- ions bind more favorably to nitrogens of PC headgroups as compared to those of TAP headgroups for all DMTAP fractions and NaCl concentrations considered here. This effect is due to the fact that small TAP headgroups are located deeper in a membrane than choline groups of DMPC lipids and, therefore, are less accessible for chloride ions.⁶ In addition, for higher DMTAP concentrations the addition of salt leads to enhanced screening away from the bilayer. That is clearly visible as the surface charge density drops much faster as a function of distance.

To conclude this discussion, it is instructive to analyze the distribution of chloride ions in the vicinity of a positively charged membrane surface using the Gouy–Chapman theory. We recall that the theory is formulated as a simple analytical

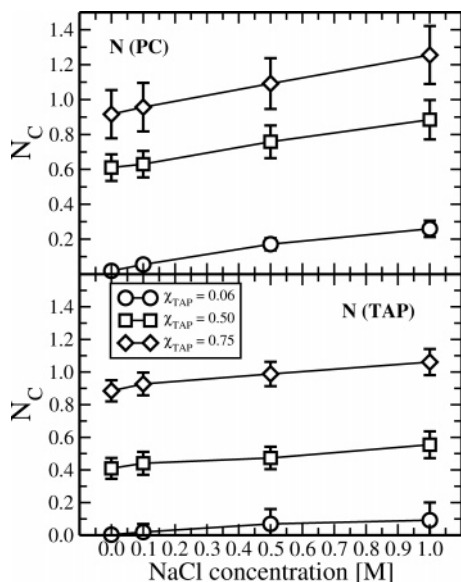


Figure 15. Coordination numbers N_C of DMPC (top) and DMTAP nitrogens (bottom) with chloride ions as a function of NaCl concentration. Shown are results for bilayers with $\chi_{TAP} = 0.06$ (circles), 0.5 (squares), and 0.75 (diamonds). The coordination numbers shown here were calculated in line with our previous study.⁶ The error bars are computed as standard deviations.

solution of the Poisson–Boltzmann equation for a cloud of counterions (with no additional salt) close to a planar, oppositely charged surface having a surface charge density σ_s ; see, e.g., ref 47 for a review. For monovalent ions the Gouy–Chapman theory predicts the following ionic number density profile

$$n_{GC}(\bar{z}) = \frac{1}{2\pi l_B} \frac{1}{(\bar{z} + b)^2} \quad (3)$$

where l_B is the Bjerrum length (equal to 0.647 nm for water at a temperature of 323 K), \bar{z} is the distance from a planar charged surface, and $b = e/2\pi l_B |\sigma_s|$ is the so-called Gouy–Chapman length.

It turns out that a proper fit of our MD results for chloride number densities becomes possible if the location of the planar charged surface is chosen to be close to DMTAP headgroup positions, i.e., to the point where DMTAP contributions to $\sigma(z)$ get saturated. This is consistent with the assumption of the Gouy–Chapman theory that the location of the planar charged surface should be determined by the surface charge density of a component whose charge is opposite to counterions. Figure 16 shows that for *salt-free* bilayer systems with medium and high DMTAP content, the MD results for number density profiles of Cl^- counterions can be fitted very well by number densities from the Gouy–Chapman theory. In Figure 16 the positions of the charged plane (dashed vertical lines) were determined from the system in the above manner; the surface charge densities σ_s used for the Gouy–Chapman theoretical curves in Figure 16 were measured directly from MD simulations as the maximal values of the DMTAP $\sigma(z)$ contributions and were taken to be $\sigma_s \approx 0.869 \text{ e/nm}^2$ for $\chi_{TAP} = 0.50$ and $\sigma_s \approx 1.216 \text{ e/nm}^2$ for $\chi_{TAP} = 0.75$. This corresponds to the Gouy–Chapman lengths of $b \approx 0.28 \text{ nm}$ and $b \approx 0.20 \text{ nm}$ for membranes with $\chi_{TAP} = 0.50$ and $\chi_{TAP} = 0.75$, respectively. For the salt-free case with $\chi_{TAP} = 0.06$, a satisfactory fitting is prohibited by insufficient sampling due to the small number of Cl^- counterions.

When salt is added, the situation becomes different. Although for bilayer systems with 0.1 M NaCl one can still have a

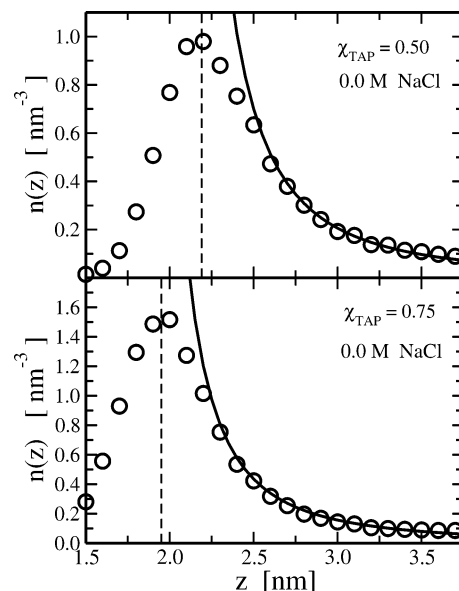


Figure 16. Fitting of number density profiles $n(z)$ of chloride ions measured in MD simulations (circles) to predictions by the Gouy–Chapman theory (solid lines) for salt-free bilayer systems with $\chi_{TAP} = 0.50$ (top) and $\chi_{TAP} = 0.75$ (bottom). The positions of planar charged surfaces used for the fitting are shown by dashed lines; see text for details.

relatively satisfactory fitting (data not shown), at higher NaCl concentrations (0.5 and 1.0 M) a proper fitting of the MD ionic number density profiles $n(z)$ by eq 3 cannot be performed. This is something what one can expect because the Gouy–Chapman theory is formulated for a situation where *only counterions* are present in a system; when electrolyte is incorporated in a system, a more involved treatment of the Poisson–Boltzmann equation in the vicinity of a planar charged surface is needed.⁴⁷

IV. Summary and Conclusions

To further our understanding of nonviral delivery vectors such as cationic liposomes, detailed atomistic studies of their properties together with complexes with DNA are called for. Such atomistic insight can be provided by “state-of-the-art” computer experiments which serve nowadays as a particularly feasible tool for studying biomolecular systems.

From this perspective, the lack of atomistic MD studies of cationic membranes is somewhat surprising. To our knowledge, the work by Bandyopadhyay et al.⁵ and our recent study of cationic salt-free DMPC/DMTAP membranes⁶ are the only exceptions to this situation. In the present work, our objective has been to provide further insight into structural and electrostatic properties of cationic membranes, focusing on the interplay of monovalent salt ions with membrane properties. In addition to all physiological cases, this issue is highly important in a variety of practical applications, including the role of electrostatic interactions in cationic lipid membranes surrounded by counterions of DNA.

We have found that the effect of monovalent NaCl on mixed DMPC/DMTAP lipid membranes depends strongly on the concentration of cationic lipids in the membrane. When the concentration is small, salt plays a major role and has a pronounced influence on the membrane. In this case the influence resembles that observed for neat zwitterionic phosphatidylcholine lipid bilayers.^{7,8,10} Sodium ions penetrate deep into the membrane and bind to the carbonyl region of DMPC lipids, while no binding of Na^+ was observed to cationic DMTAP. The formation of sodium-induced complexes between

DMPC lipids leads to a considerable compression of a membrane and to a concurrent enhancement of the ordering of nonpolar hydrocarbon chains for both DMPC and DMTAP. Furthermore, sodium ions give rise to a reorientation of zwitterionic PC headgroups in the outward direction of the bilayer, which results in a slight increase of the total electrostatic potential across a monolayer.

In contrast, cationic membranes with medium and high DMTAP content ($\chi_{\text{TAP}} \geq 0.50$) turn out to be very robust to monovalent salt. This fact originates from a substantial positive surface charge of the membranes, which prevents the binding of sodium ions to DMPC carbonyl oxygens located deep in the membrane. As a critical test of our conclusions, one of the simulations for a membrane containing an equimolar DMPC/DMTAP mixture was extended to 200 ns and no stable binding of Na^+ ions to the membrane was found. Thus, mixed cationic/zwitterionic lipid membranes containing a substantial fraction of cationic lipids are found to be almost insensitive to *monovalent* salt. However, as our ongoing studies demonstrate, this is not the case for *divalent* salt.

To some extent, the above results for cationic membranes in aqueous salt solution may shed light on the problem of the influence of counterions of DNA on the properties of cationic membranes and, perhaps, on the formation of complexes comprised of DNA and cationic lipids. Whether or not the role of the DNA counterions is insignificant when membranes contain a substantial fraction of cationic lipids has to be resolved directly through systematic MD simulation studies of DNA–cationic membrane complexes. We defer such studies to our future work.

Acknowledgment. Fruitful discussions with P. Niemelä and M. Patra are gratefully acknowledged. Special thanks go to I. Degtyarenko for technical support. This work has been supported by the Academy of Finland through Grants. 202598 (A.A.G.), 80246 (I.V.), 54113 (M.K. and M.M.), and 00119 (M.K.), and by its Center of Excellence Program. The simulations were performed on the IBM supercomputer at the Finnish IT Center for Science (CSC) and on the HorseShoe (DCSC) supercluster at the University of Southern Denmark.

References and Notes

- (1) Lasic, D. D. *Liposomes in Gene Delivery*; CRC Press: Boca Raton, FL, 1997.
- (2) Lasic, D. D.; Strey, H.; Stuart, M. C.; Podgornik, R.; Frederik, P. M. *J. Am. Chem. Soc.* **1997**, *119*, 832.
- (3) Rädler, J. O.; Koltover, I.; Salditt, T.; Safinya, C. R. *Science* **1997**, *275*, 810.
- (4) Pitard, B.; Aguerre, O.; Airiau, M.; Lachages, A. M.; Boukhnikachvili, T.; Byk, G.; Dubertret, C.; Herviou, C.; Scherman, D.; Mayaux, J. F.; Crouzet, J. *Proc. Natl. Acad. Sci. U.S.A.* **1997**, *94*, 14412.
- (5) Bandyopadhyay, S.; Tarek, M.; Klein, M. L. *J. Phys. Chem. B* **1999**, *103*, 10075.
- (6) Gurtovenko, A. A.; Patra, M.; Karttunen, M.; Vattulainen, I. *Biophys. J.* **2004**, *86*, 3461.
- (7) Böckmann, R. A.; Hac, A.; Heimburg, T.; Grubmüller, H. *Biophys. J.* **2003**, *85*, 1647.
- (8) Böckmann, R. A.; Grubmüller, H. *Angew. Chem., Int. Ed.* **2004**, *43*, 1021.
- (9) Pandit, S. A.; Bostick, D.; Berkowitz, M. L. *Biophys. J.* **2003**, *84*, 3743.
- (10) Gurtovenko, A. A. *J. Chem. Phys.* **2005**, *122*, 244902.
- (11) Pandit, S. A.; Berkowitz, M. L. *Biophys. J.* **2002**, *82*, 1818.
- (12) Pandit, S. A.; Bostick, D.; Berkowitz, M. L. *Biophys. J.* **2003**, *85*, 3120.
- (13) Mukhopadhyay, P.; Monticelli, L.; Tieleman, D. P. *Biophys. J.* **2004**, *86*, 1601.
- (14) McLaughlin, S. *Annu. Rev. Biophys. Biophys. Chem.* **1998**, *18*, 113.
- (15) Cevc, G. *Biochim. Biophys. Acta* **1990**, *1031*, 311.
- (16) Tatulian, S. A. Ionization and ion binding. In *Phospholipids Handbook*; Cevc, G., Ed.; Marcel Dekker: New York, 1993; p 511.
- (17) Binder, H.; Zschörnig, O. *Chem. Phys. Lipids* **2002**, *115*, 39.
- (18) Tatulian, S. A. *Eur. J. Biochem.* **1987**, *170*, 413.
- (19) Gunningham, B. A.; Gelerinter, E.; Lis, L. J. *Chem. Phys. Lipids* **1988**, *46*, 205.
- (20) Roux, M.; Bloom, M. *Biochemistry* **1990**, *29*, 7077.
- (21) Clarke, R. J.; Lüpfer, C. *Biophys. J.* **1999**, *76*, 2614.
- (22) Rappolt, M.; Pabst, G.; Amenitsch, H.; Laggner, P. *Colloids Surf., A* **2001**, *183*, 171.
- (23) Ohki, S.; Arnold, K. *Colloids Surf., B* **2000**, *18*, 83.
- (24) Artzner, F.; Zantl, R.; Rapp, G.; Rädler, J. O. *Phys. Rev. Lett.* **1998**, *81*, 5015.
- (25) Zantl, R.; Artzner, F.; Rapp, G.; Rädler, J. O. *Europhys. Lett.* **1999**, *45*, 90.
- (26) Zantl, R.; Baicu, L.; Artzner, F.; Sprenger, I.; Rapp, G.; Rädler, J. O. *J. Phys. Chem. B* **1999**, *103*, 10300.
- (27) Pohle, W.; Selle, C.; Gauger, D. R.; Zantl, R.; Artzner, F.; Rädler, J. O. *Phys. Chem. Chem. Phys.* **2000**, *2*, 4642.
- (28) Berger, O.; Edholm, O.; Jahnig, F. *Biophys. J.* **1997**, *72*, 2002.
- (29) Tieleman, D. P.; Berendsen, H. J. C. *J. Chem. Phys.* **1996**, *105*, 4871.
- (30) Lindahl, E.; Edholm, O. *Biophys. J.* **2000**, *79*, 426.
- (31) Nagle, J. F.; Wiener, M. C. *Biochim. Biophys. Acta* **1988**, *942*, 1.
- (32) Berendsen, H. J. C.; Postma, J. P. M.; van Gunsteren, W. F.; Hermans, J. Interaction models for water in relation to protein hydration. In *Intermolecular Forces*; Pullman, B., Ed.; Reidel: Dordrecht, 1981; p 331.
- (33) Berendsen, H. J. C.; van der Spoel, D.; van Drunen, R.; *Comput. Phys. Commun.* **1995**, *91*, 43.
- (34) Lindahl, E.; Hess, B.; van der Spoel, D. *J. Mol. Model.* **2001**, *7*, 306.
- (35) Patra, M.; Karttunen, M. *J. Comput. Chem.* **2004**, *25*, 678.
- (36) Patra, M.; Karttunen, M.; Hyvönen, M. T.; Falck, E.; Lindqvist, P.; Vattulainen, I. *Biophys. J.* **2003**, *84*, 3636.
- (37) Anézo, C.; de Vries, A. H.; Höltje, H. D.; Tieleman, D. P.; Marrink, S. J. *J. Phys. Chem. B* **2003**, *107*, 9424.
- (38) Patra, M.; Karttunen, M.; Hyvönen, M. T.; Falck, E.; Vattulainen, I. *J. Phys. Chem. B* **2004**, *108*, 4485.
- (39) Darden, T.; York, D.; Pedersen, L. J. *J. Chem. Phys.* **1993**, *98*, 10089.
- (40) Essman, U.; Perera, L.; Berkowitz, M. L.; Darden, T.; Lee, H.; Pedersen, L. G. *J. Chem. Phys.* **1995**, *103*, 8577.
- (41) Berendsen, H. J. C.; Postma, J. P. M.; van Gunsteren, W. F.; DiNola, A.; Haak, J. R. *J. Chem. Phys.* **1984**, *81*, 3684.
- (42) Hess, B.; Bekker, H.; Berendsen, H. J. C.; Fraaije, J. G. E. M. *J. Comput. Chem.* **1997**, *18*, 1463.
- (43) Miyamoto, S.; Kollman, P. A. *J. Comput. Chem.* **1992**, *13*, 952.
- (44) Säily, V. M. J.; Alakoskela, J. M.; Ryhänen, S. J.; Karttunen, M.; Kinnunen, P. K. *J. Langmuir* **2003**, *19*, 8956.
- (45) Chiu, S. W.; Clark, M.; Balaji, V.; Subramaniam, S.; Scott, H. L.; Jacobsson, E. *Biophys. J.* **1995**, *69*, 1230.
- (46) Hofsäas, C.; Lindahl, E.; Edholm, O. *Biophys. J.* **2003**, *84*, 2192.
- (47) Andelman, D. Electrostatic Properties of Membranes: The Poisson–Boltzmann Theory. In *Handbook of Biological Physics*; Lipowsky, R., Sackmann, E., Eds.; Elsevier Science: Amsterdam, 1995; p 603.